Effect of electron-to-ion mass ratio on radial electric field generation in tokamak

Zhenqian Li[1], Jiaqi Dong[2,1], Zhengmao Sheng[1], M. Y. Yu[1,3] and Weixing Wang[4]

[1]Institute for Fusion Theory and Simulation and Department of Physics, Zhejiang University, Hangzhou 310027, China
[2] Southwest Institute of Physics, Chengdu 610041, China
[3] Institute for Theoretical Physics I, Ruhr University, Bochum D-44780, Germany
[4]Princeton Plasma Physics Laboratory, Princeton University, P. O. Box 451, Princeton, New Jersey, 08543, USA

E-mail: zmsheng@zju.edu.cn

Abstract. Generation of zonal radial electric fields in tokamak plasma by drift-wave turbulence, in particular, the effect of the electron-to-ion mass ratio ϵ on the entire evolution of the plasma, is studied using gyro-kinetic particle simulation. It is shown that the zonal electric field can be enhanced, and the turbulence-induced transport reduced, by making ϵ smaller, in agreement with the experimental observations.

PACS numbers: 52.35.Ra, 52.55.Fa, 52.35.Kt

1. Introduction

In magnetic confinement of plasma, anomalous transport of particles and heat can be driven by plasma turbulence [1]. To achieve fusion energy gain, effective suppression or control of the anomalous transport is necessary. The ubiquitous drift-wave instabilities and resulting turbulence arising from plasma inhomogeneity induced instabilities have been considered as a major cause of the transport [2]. On the other hand, coherent radial electric fields (E_r) generated from self organization of the turbulent drift waves can lead to poloidal, or zonal, flows that in turn suppress the turbulence and the anomalous radial transport, thereby improving plasma confinement [3, 4]. In this paper we investigate the process of E_r generation by means of gyro-kinetic particle simulation, starting with the initial stage of excitation of trapped electron mode (TEM) drift waves and their nonlinear growth, followed by and onset of turbulence and coherent radial electric fields generation, until a quasi-stationary state of low-level turbulence and low radial particle fluxes appears because of a balance between the energy input and dissipation via Landau damping and flow friction. However, the coherent radial electric field can continue to grow since it can still be fed by the free energy of the plasma inhomogeneities (whose relaxation time is much longer that involved in the zonal flow generation process

considered here). In particular, the isotope effect, or that of the electron-to-ion mass ratio $\epsilon = m_e/m_i$, is considered. It is found that, as observed in existing experiments [5], by reducing ϵ, E_r can be increased and the drift turbulence and anomalous radial transport reduced.

2. Problem formulation and simulation

To get an overall picture, we shall track the entire evolution process, namely from the TEM drift-wave instability to the onset and evolution of drift-wave turbulence, and to the eventual quasistationary zonal-flow state, where the free energy from the plasma inhomogeneity continuously feeds the zonal flow via low-level quasistationary drift-wave turbulence, accompanied by low-level plasma transport. For our investigation, we shall use the gyro-kinetic particle simulation code GTS [6] and typical plasma parameters of an L-mode phase of the Alcator C-Mod tokamak [7, 8]. The GTS code performs global, five-dimensional gyrokinetic simulations of the dynamics of the waves, particles, as well as their linear and nonlinear interactions in tokamak plasma, and is thus especially suitable for investigating turbulent transport [6, 9]. The C-Mod tokamak has major radius $R_0 = 0.67$m and minor radius $a = 0.22$m. The radial domain of our interest is $0.3 < r/a < 0.9$. The full profiles of the initial parameters (especially the magnetic field distribution) used in our simulations are generated from the C-Mod parameters by the ESC code [10]. The toroidal magnetic field on the magnetic axis is $B_0 = 5.8$T. Figure 1 shows the profiles of the plasma density n_0, and the ion and electron temperatures T_i and T_e. In this plasma configuration, the ion temperature gradient is relatively weak, and we are well in the unstable TEM regime. Accordingly, the TEM instability dominates and it can drive the resulting drift-wave turbulence throughout our simulation.

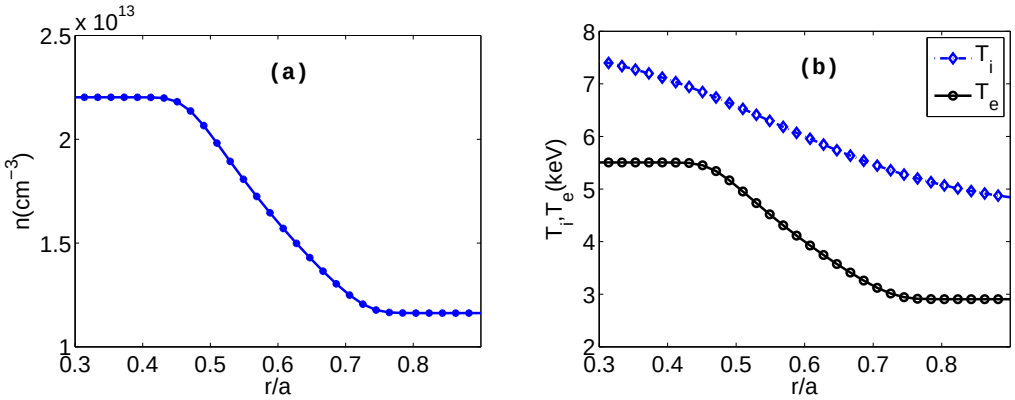

Figure 1. (Color online.) Initial radial profiles of the (a) electron (or ion) density $n(r)$, and (b) electron and ion temperatures T_e and T_i, respectively.

It is now well known that coherent quasi-steady radial electric fields can be induced by neoclassical effects as well as drift-wave turbulence [11]. In our simulation, the initial particle distribution is locally Maxwellian and thus not in neoclassical equilibrium

[6]. As a result, a radial electric field is self-consistently generated after the start of the simulation. To see this neoclassical process more clearly, we first consider a case with very small initial density and temperature gradients, so that drift-wave effects are negligible. Figure 2(a) for deuterium plasma shows the evolution of the self-generated radial electric field E_r, and (b) more clearly its oscillatory behavior at $r/a = 0.6$. The period of the oscillations is roughly $7L_n/v_{thi} \sim 3.5\mu$sec. As expected, E_r appears as soon as the simulation starts, and it oscillates at the frequency of the geodesic acoustic mode (GAM) [12, 13]. Here the GAM is Landau damped since T_i and T_e are of the same order [13], so that after a few oscillations a steady E_r remains, establishing a neoclassical equilibrium [14].

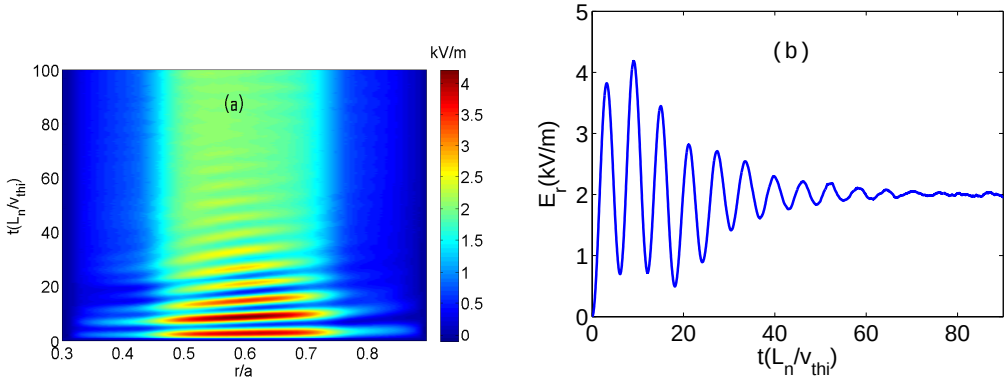

Figure 2. (Color online.) (a) Evolution of the radial electric field E_r induced by neoclassical effects only. (b) E_r at $r/a = 0.6$. The time is in units of L_n/v_{thi} ($\sim 0.5\mu$sec for the parameters here), where L_n and v_{thi} are the density scale length and ion thermal speed, respectively.

On the other hand, if we start with the equilibrium profiles shown in figure 1, unstable drift waves are excited because of the TEM instability [15, 16], which then results in drift-wave growth, modulation, and turbulence. Because of the initial neoclassical stage, the E_r generated by the drift waves and the resulting turbulence would appear as a second stage of its evolution, in which the original neoclassical E_r are enhanced, i.e., E_r starts to grow again. This process can be seen in figure 3 for the evolution of E_r, the intensity of the drift waves as given by the electrostatic potential $|\tilde{\phi}| = \langle\sqrt{|\phi - \langle\phi\rangle|^2}\rangle$, where the angular brackets denote averaging over the magnetic surface, as well as the radial ion flux Γ_i. We can see that drift waves start to grow at $t \lesssim 50$ and they become fully turbulent at $t \gtrsim 70$. After a stage of unsteady development involving competition among nonlinear mechanisms such as wave-wave and wave-particle and particle-particle (i.e., collisions) interactions, the turbulence becomes damped and eventually saturates at a low level. As expected, the evolution of Γ_i is similar. The relatively coherent E_r generated by self-organization (namely inverse cascade to longer-wavelength modes) of the turbulent drift waves. It saturates at a much later time (not shown) since the free energy of the plasma inhomogeneities (as long as they remain sufficiently large) can still be converted to it via the drift-wave turbulence,

which however remains steady. The corresponding poloidal zonal plasma flow E_r/B_0 can also contribute to the energy dissipation via collisional damping. Moreover, the fact that $|\tilde{\phi}|$ and Γ_i are strongly correlated throughout the turbulent stage ($t \gtrsim 70$) confirms that the radial ion flux is also ponderomotively driven by the drift-wave turbulence [17, 18, 19]. For the same reason, one can expect that the ϵ, or the isotope effect, can play an important role in the generation and evolution of the radial electric field, and therefore also the onset of the L- to H-mode transition. [5, 20, 21, 22, 23].

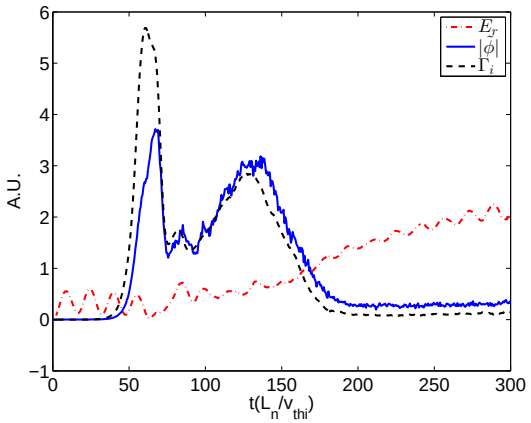

Figure 3. (Color online.) Evolution of the averaged (over the simulated magnetic surface) electrostatic potential $|\tilde{\phi}|$ of the drift waves, the self-organized radial electric field E_r, and the ion flux Γ_i. The process starts with the neoclassical stage, where $|\tilde{\phi}| = 0$, $\Gamma_i = 0$, and GAM is generated. As the second stage, drift-wave instability and drift-wave turbulence occur at $t \lesssim 50$ (linear growth) and $t \sim 70$, respectively, followed by competing wave-wave, wave-particle, and particle-particle (collisional friction in the sheared zonal flow) interactions. At $t \gtrsim 250$, a quasi-steady low-level turbulent state with roughly constant Γ_i and time-averaged $|\tilde{\phi}|$, but a steadily growing (roughly linear in time) E_r, appears. The strong correlation between $|\tilde{\phi}|$ and Γ_i suggests that the ion flow is ponderomotively driven by the drift-wave turbulence.

3. Mass-ratio effects

Accordingly, we next investigate the mass-ratio effect on the evolution of the radial electric field E_r, the ion and electron fluxes Γ_i and Γ_e, and the electrostatic fluctuation potential $|\tilde{\phi}|$ by considering three cases: $\epsilon = 1/3684$ (deuterium plasma), $\epsilon = 1/1879$ (hydrogen plasma), and $\epsilon = 1/919$ (a fictitious case for checking what happens if the ion mass is very small). To save computation time, in the simulation the different cases are realized by scaling the unit of m_e, keeping the ion mass number fixed at 3674 for deuterium. Such a representation is valid here since in the simulation code the full kinetic equations for both electrons and ions are solved. The evolution of the radial electric field E_r at $r/a = 0.6$ (where the electron density and temperature gradients are maximum) is shown in figure 4(a).In the figure, the time is normalized by L_n/v_{thi}, which is proportional to $m_i^{1/2}$. That is, in view of our rescaling of m_e for simulating the

dynamics of the hydrogen and fictitious ions, in the figure the time coordinates for the latter have been shrunk by a factor of $1/\sqrt{2}$ and $1/\sqrt{4}$, respectively. This manipulation has the advantage (for the purpose of comparison) that the resulting curves, as well as their different evolution stages, are roughly located in the same time domains in the figure. For example, in this representation the initial neoclassical electric fields oscillations for the three ion species fully overlap, consistent with the fact that their periods should differ by exactly $1/\sqrt{m_i}$ and that their magnitudes do not depend on the ion mass [14, 24]. After $t = 50$, unstable drift waves are excited. As the waves grow, E_r is enhanced and modulated until the onset of drift-wave turbulence, and energy redistribution and dissipation enhancement occur [25]. It is of interest to note that the oscillations first appearing in the neoclassical stage are superposed on the growing E_r throughout the evolution, with the (normalized for each species) period apparently unchanged and independent of ϵ. This can be attributed to the fact that such GAM-like oscillations should depend only on the mode number, the plasma radius, and the ion acoustic speed. But here the latter is included in the time normalization (recall that the initial T_i and T_e are fixed at 6keV 4keV, respectively). It is also of interest to note that the amplitude of the oscillations is largest for the intermediate mass (hydrogen) case. Figure 4(b) shows the radial profile of the time-averaged (over $250 < t < 300$, same in the following, unless otherwise stated) E_r. One can see that for the case of small mass ratio (fictitious light ions), the radial electric field E_r is considerably less but multi peaked, and more localized and radially inward shifted.

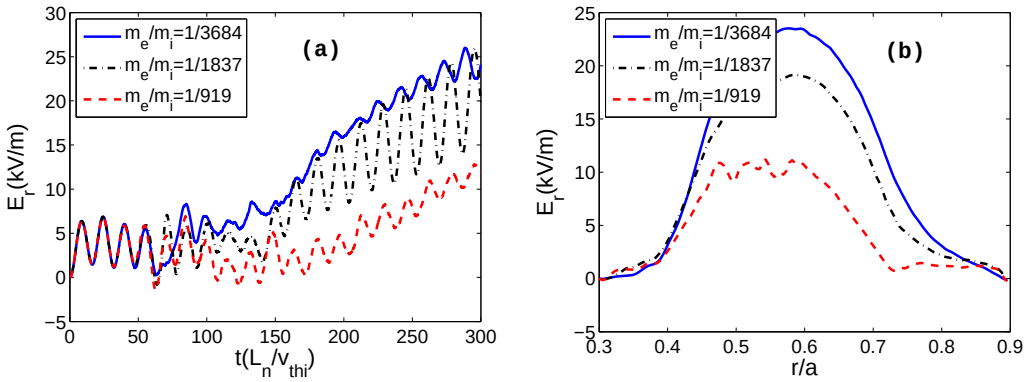

Figure 4. (Color online.)(a) Evolution of the radial electric field E_r for $\epsilon = 1/3684$ (hydrogen), 1/1879 (deuterium), and 1/919 (a fictitious case). Note that E_r does not depend on ϵ in the neoclassical stage $0 < t < 50$. Moreover, its oscillation period remains unchanged at all times. (b) The time-averaged (over the period $250 < t < 300$, same in the following figures unless otherwise stated) radial profile of E_r. One can see that E_r (and thus the corresponding zonal flow magnitude E_r/B_0) is larger and more localized for the heavier ions.

The evolution of the ion and electron fluxes Γ_i and Γ_e as functions of ϵ are shown in figure 5. We can see that smaller ϵ corresponds to smaller radial particle fluxes. Moreover, (in view of the time normalization for each ϵ value) all the fluxes start to grow at $t \sim 50$, peaking at different times, and then they all decrease rapidly, reaching

their steady-state low levels at $t \sim 250$. The fact that in the initial neoclassical stage there are no such particle fluxes, and that their evolution behavior roughly follow that of the averaged drift-wave potential fluctuations (to be shown below), indicate that the fluxes are driven by the unstable, modulated, and then turbulent drift waves. The behavior of the electron and ion radial fluxes are nearly the same, with small differences when (and shortly after) the drift waves become turbulent at $t \sim 70$.

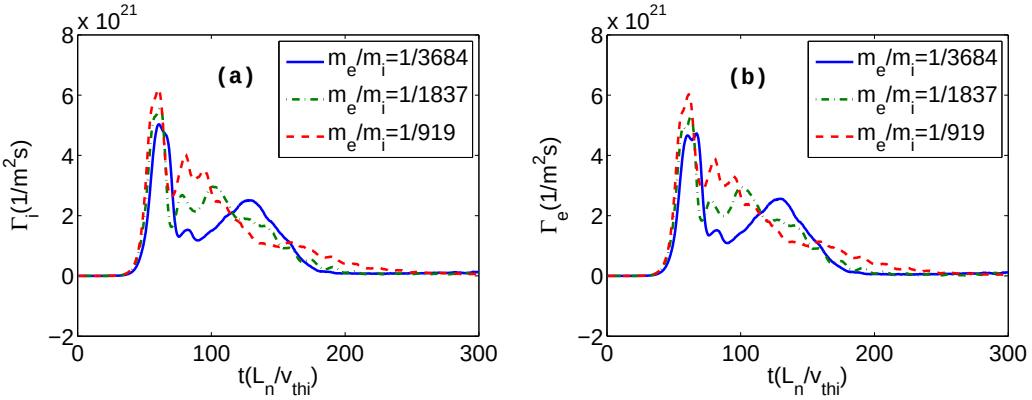

Figure 5. (Color online.) Evolution of the radial (a) ion flux Γ_i and (b) electron flux Γ_e. Note that the difference between the ion and electron fluxes of the same ion species is small.

Figure 6(a) shows the evolution of the intensity of the drift-wave fluctuations as given by the magnetic-surface averaged electrostatic fluctuation potential $|\tilde{\phi}|$. In contrast to that of E_r and $\Gamma_{i,e}$, one can see that $|\tilde{\phi}|$ is smallest and least peaked for the most massive (deuterium) ions. Moreover, the evolution of $\Gamma_{i,e}$ closely follow that of $|\tilde{\phi}|$, but the growth of E_r is much less sensitive to the details of $|\tilde{\phi}|$, especially in the stormy predator-prey stage $70 < t < 170$. This behavior suggests that the drift-wave fluctuations are driving the particle fluxes and the radial electric field through different channels, which is even more evident at later times ($t > 170$), when E_r grows but $|\tilde{\phi}|$ and $\Gamma_{i,e}$ have become quasi-steady.

The evolution behavior of the parameters discussed above are consistent with the prevailing paradigm for the physics of drift-wave turbulence and zonal flow generation [26]. It is thus of interest to see how does the ion mass relate to the parameters considered in a time interval relevant to the main evolution stage. Figure 7 shows the dependence of the time-averaged (over $50 < t < 250$, i.e., when drift waves are active. Recall that in real time this period would be $50 \times \sqrt{2} < t\ [L/v_{thd}] < 250 \times \sqrt{2}$ and $50 \times 2 < t\ [L/v_{thd}] < 250 \times 2$ for the hydrogen and fictitious ions, respectively, where v_{thd} is the thermal speed of the deuterium ions) (a) E_r, (b) Γ_i and Γ_e, and (c) $|\tilde{\phi}|^2$ on the mass ratio ϵ at $r/a = 0.6$, where the electron density and temperature gradients are maximum. We see that all the curves are straight or nearly straight lines and that larger ion mass leads to lower levels of drift-wave turbulence and radial transport, but larger zonal radial electric fields. However, it should be noted that if these parameters were averaged over other time domains, the curves may not be straight (or even nearly

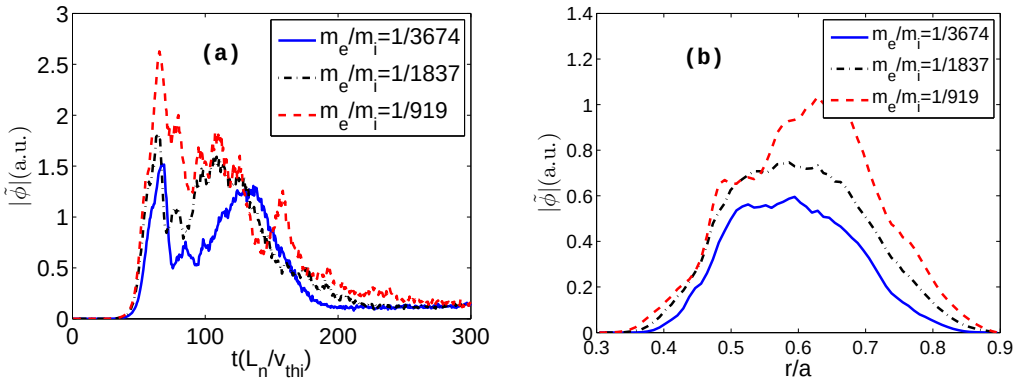

Figure 6. (Color online.) (a) Evolution of the drift-wave potential $|\tilde{\phi}|$ for the 3 different mass ratios. (b) The corresponding time-averaged (over $50 < t < 250$) $|\tilde{\phi}|$ at $r/a = 0.6$.

straight) lines. For example, if the averaging were over $50 < t < 100$ (i.e., the most unsteady regime of the evolution for each ion species), we found that (not shown) only the curve for $|\tilde{\phi}|^2$ versus ϵ remains a straight line. This suggests that even in this unsteady domain, $|\tilde{\phi}|^2$ scales linearly with m_i^{-1}, which in turn can suggest that in the process the time-integrated generalized enstrophy [27] is conserved [28]. On the other hand, our simulations include in detail processes such as Landau damping, particle collisions, particle trapping, etc. that are ignored in the paradigm drift-wave turbulence theories. Thus, the results here suggest that enstrophy conservation may be robust for drift-wave turbulence in tokamak plasma. However, for a definitive conclusion, a more detailed theoretical justification (beyond that of the ion-mass dependence of the enstrophy) would be needed.

4. Discussion and Summary

Electron and ion transport in drift-wave turbulence have also been investigated by following the trajectories of test particles [29, 30]. It was found that the turbulence level can play important roles. These observations are consistent with our simulation result that the particle fluxes are affected by the mass ratio and the turbulence intensity. The results of our simulations on the mass-ratio effect are consistent with that of the recent studies on the isotope effect on the zonal flow and the L-H mode transition [5, 21, 22, 31, 32], where it was found that, compared with that for hydrogen plasma, for deuterium plasma the zonal field is larger and the confinement properties better.

In summary, we have investigated by gyrokinetic simulation the effect of the plasma particle mass ratio on the full evolution process: from the formation of the neoclassical stage, the TEM instability and the subsequent drift-wave turbulence, energy redistribution, dissipation, self-organization, and asymptotically arriving at a quasistationary state involving low levels of turbulence and radial particle fluxes. The latter state is due to self-organization of the drift-wave turbulence, where some of the

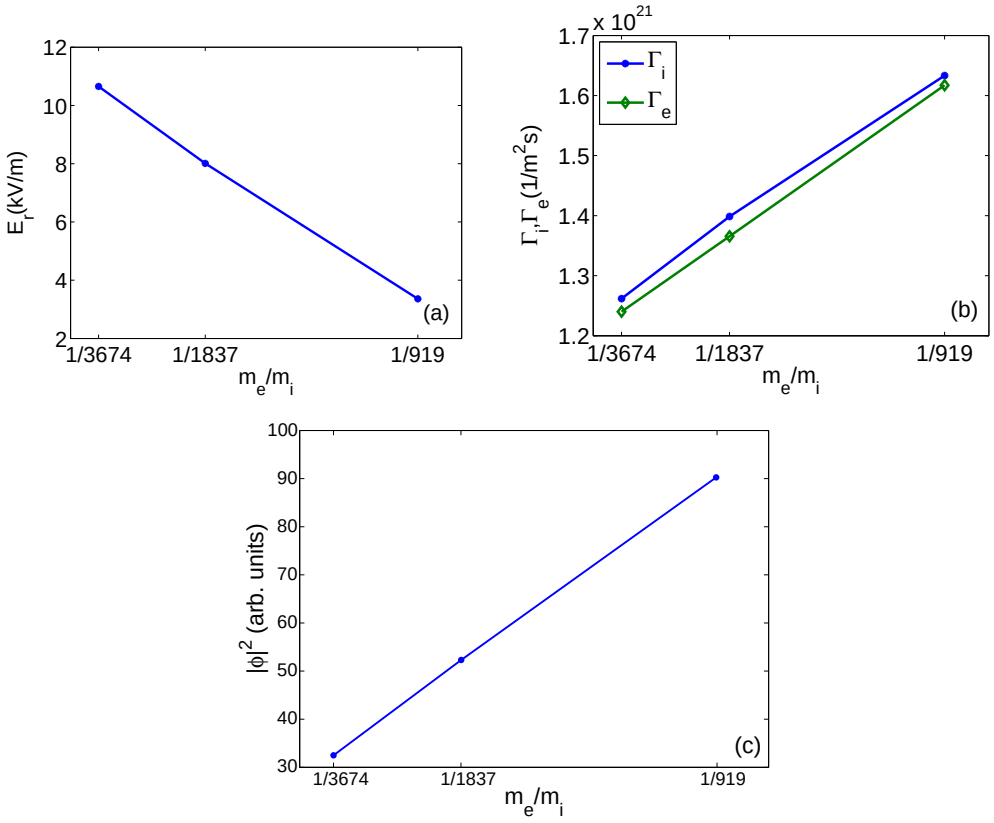

Figure 7. (Color online.) Time averaged (over $50 < t < 250$) (a) radial electric field E_r, (b) radial ion and electron fluxes Γ_i and Γ_e, and (c) intensity $|\tilde{\phi}|^2$ of the drift-wave fluctuation potential versus ϵ at $r/a = 0.6$.

energy is inverse-cascaded to the longer wavelengths, thereby giving rise to coherent radial electric field and particle fluxes. The quasistationary state appears because of a dynamic balance between the energy (from the free energy of the density and temperature gradients) input and energy dissipation via Landau damping (of the drift waves) and particle collisions (of the sheared zonal flow). However, the radial electric field and thus the poloidal zonal flow continue to grow via energy transfer through the low-level drift-wave turbulence, since the initial plasma density and temperature gradients (recall that they are far from the marginal TEM instability condition) constitute a huge energy reservoir in our simulation. It is also shown that smaller ϵ leads to larger radial electric field E_r and thus stronger zonal flow, and asymptotically smaller turbulence level and smaller particle fluxes, which should be beneficial to the L-H transition and plasma confinement [26]. Moreover, our results suggest that enstrophy conservation may be robust in the evolution of drift wave turbulence in tokamak plasma.

Acknowledgments

We thank Weiwen Xiao for useful discussions. This work has been supported by the National Magnetic Confinement Fusion Program under grant nos. 2013GB104004 and

2013GB111004, the National Natural Science Foundation of China (NSFC) under grant nos. 11235009 and 11374262, the Fundamental Research Fund for Chinese Central Universities under grant no. 2016FZA3003, and the Open Fund of the State Key Laboratory of High-Field Laser Physics at SIOM.

References

[1] Horton W 1999 *Rev. Mod. Phys.* **71** 735
[2] Mazzucato E 1976 *Phys. Rev. Lett.* **36** 792–4
[3] Lin Z, Hahm T S, Lee W W, Tang W M and White R B 1998 *Science* **281** 1835
[4] Hidalgo C, Silva C, Pedrosa M A, Sanchez E, Fernandes H and Varandas C A F 1999 *Phys. Rev. Lett.* **83** 2203–5
[5] Xu Y, Hidalgo C, Shesterikov I, Kramerflecken A, Zoletnik S, M V S, Vergote M and Team T 2013 *Phys. Rev. Lett.* **110** 265005
[6] Wang W, Lin Z, Tang W, Lee W, Ethier S, Lewandowski J, Rewoldt G, Hahm T and Manickam J 2006 *Phys. Plasmas* **13** 092505
[7] Hutchinson I, Boivin R, Bombarda F, Bonoli P, Fairfax S, Fiore C, Goetz J, Golovato S, Granetz R, Greenwald M *et al.* 1994 *Phys. Plasmas* **1** 1511–8
[8] Scott S D, Bader A, Bakhtiari M, Basse N P, Beck W K, Biewer T M, Bernabei S, Bonoli P T, Bose B, Bravenec R V *et al.* 2007 *Nucl. Fusion* **49** 104014
[9] Wang W, Diamond P, Hahm T, Ethier S, Rewoldt G and WM T 2010 *Phys. Plasmas* **17** 072511
[10] Zakharov L and Pletzer A 1999 *Phys. Plasmas* **6** 4693–704
[11] Novakovskii S, Liu C, Sagdeev R and Rosenbluth M 1997 *Phys. Plasmas* **4** 4272–82
[12] Winsor N, Johnson J L and Dawson J M 1968 *Phys. Fluids* **11** 2448–50
[13] Sugama H and Watanabe T H 2006 *J. Plasma Phys.* **72** 825–8
[14] Wessen J 2004 *Tokamaks, 3rd Edition* (Cambridge University Press, Cambridge, UK)
[15] Adam J C, Tang W M and Rutherford P H 1976 *Phys. Fluids* **19** 561–6
[16] Ryter F, Angioni C, Peeters A G, Leuterer F, Fahrbach H U, Suttrop W and Team A U 2005 *Phys. Rev. Lett.* **95** 085001
[17] Vedenov A, Gordeev A and Rudakov L 1967 *Plasma Phys.* **9** 719
[18] Smolyakov A, Diamond P and Medvedev M 2000 *Phys. Plasmas* **7** 7
[19] Zakharov L and Pletzer A 1999 *Phys. Plasmas* **6** 4693–704
[20] Dong J Q, Horton W and Dorland W 1994 *Phys. Plasmas* **1** 3635–40
[21] Bessenrodt-Weberpals M, Wagner F, Gehre O, Giannone L, Hofmann J, Kallenbach A, McCormick K, Mertens V, Murmann H, Ryter F, Scott B, Siller G, Soldner F, Stabler A, Steuer K H, Stroth U, Tsois N, Verbeek H and Zoohm H 1993 *Nucl. Fusion* **33** 1205
[22] Hahm T S, Wang L, Wang W, Yoon E and Duthoit F 2013 *Nucl. Fusion* **53** 072002
[23] Shen Y, Dong J Q, Sun A P, Qu H P, Lu G M, He Z X, He H D and Wang L F 2016 *Plasma. Phys. Contr. Fusion* **58** 045028
[24] Wang W X, Hinton F L and Wong S K 2001 *Phys. Rev. Lett.* **87** 055002
[25] Scott B D 2002 *New J. Phys.* **4** 52
[26] Diamond P, Itoh S, Itoh K and Hahm T 2005 *Plasma. Phys. Contr. Fusion* **47** 5
[27] Hasegawa A and Mima K 1978 *Phys. Fluids* **21**, 87
[28] In the wavevector space the enstrophy is proportional to [27] $\sum_{\boldsymbol{k}} |\boldsymbol{k}|^2\rho^2(1+|\boldsymbol{k}|^2\rho^2)|\tilde{\phi}_{\boldsymbol{k}}|^2$, where $\boldsymbol{k}$ is the wave vector of the drift waves and ρ_s the ion gyroradius in terms of the electron temperature. Since in the tokamak the drift-wave fluctuations are mainly of long wavelengths, or $|\boldsymbol{k}|\rho_s \ll 1$, enstrophy conservation leads to $|\tilde{\phi}_{\boldsymbol{k}}|^2 \propto \rho_s^2 \propto 1/m_i$.
[29] Vlad M, Spineanu F, Itoh S, Yagi M and Itoh K 2005 *Plasma Phys. Contr. Fusion* **47** 1015
[30] Zhang W, Lin Z, Chen L 2008 *Phys. Rev. Lett.* **101** 095001
[31] Stroth U 1998 *Plasma Phys. Contr. Fusion* **40** 9

[32] Ryter F, Putterich T, Reich M, Scarabosio A, Wolfrum E, Fischer R, Adamov M G, Hicks N, Kurzan B, Maggi C F *et al.* 2009 *Nucl. Fusion* **49** 062003